Journal of Bioscience and Bioengineering
VOL. 127 No. 5, 563–569, 2019

www.elsevier.com/locate/jbiosc

Kinetic modeling and sensitivity analysis for higher ethanol production in self-cloning xylose-using *Saccharomyces cerevisiae*

Akira Fukuda,[1,2] Yuki Kuriya,[1] Jin Konishi,[2] Kozue Mutaguchi,[2] Takeshi Uemura,[2] Daisuke Miura,[3] and Masahiro Okamoto[4,*]

Laboratory of Synthetic Biology, Graduate School of Bioresource and Bioenvironmental Science, Kyushu University, 3-1-1 Maidashi, Higashi-ku, Fukuoka 812-8582, Japan,[1] Biofuel R&D Group, Frontier Research Laboratory, Central Technical Research Laboratory, JXTG Nippon Oil & Energy Corporation, 8 Chidoricho, Naka-ku, Yokohama 231-0815, Japan,[2] Metabolic Profiling Research Group, Innovation Center for Medical Redox Navigation, Kyushu University, 3-1-1 Maidashi, Higashi-ku, Fukuoka 812-8582, Japan,[3] and Laboratory of Synthetic Biology, Graduate School of Systems Life Sciences, Kyushu University, 3-1-1 Maidashi, Higashi-ku, Fukuoka 812-8582, Japan[4]

Received 17 September 2018; accepted 25 October 2018
Available online 24 November 2018

We constructed a xylose-utilizing *Saccharomyces cerevisiae* strain using endogenous xylose-assimilating genes (strain K7-XYL). Such self-cloning yeast is expected to make a great contribution to cost reduction of ethanol production processes. However, it is difficult to modify self-cloning yeast for optimal performance because the available gene source is limited. To improve the ethanol productivity of our self-cloning yeast, a kinetic model of ethanol production was constructed and sensitivity analysis was performed. Alcohol dehydrogenase (*ADH1*) was identified as a metabolic bottleneck reaction in the ethanol production pathway. An *ADH1* overexpression strain (K7-XYL-ADH1) was constructed and evaluated in YP (yeast extract 10 g/L, peptone 20 g/L) medium containing 50 g/L xylose as the sole carbon source. Strain K7-XYL-ADH1 showed higher ethanol productivity (13.8 g/L) than strain K7-XYL (12.5 g/L). Then, K7-XYL-ADH1 was evaluated in YP medium containing 80 g/L glucose and 50 g/L xylose; however, the ethanol productivity did not change relative to that of K7-XYL (K7-XYL 46.3 g/L, K7-XYL-ADH1 45.9 g/L). We presumed that due to the presence of glucose, the internal redox balance of the cells had changed. On culturing in an aerated 5-L jar fermentor to change the internal redox balance of cells, strain K7-XYL-ADH1 showed higher ethanol productivity than K7-XYL (K7-XYL 45.0 g/L, K7-XYL-ADH1 49.4 g/L). Our results confirmed that ADH1 was a metabolic bottleneck in the ethanol production pathway. By eliminating the bottleneck, self-cloning yeast showed almost the same ethanol productivity as genetically modified yeast.

[**Key words:** *Saccharomyces cerevisiae*; Self-cloning; Ethanol production; Xylose; Kinetic modeling; Metabolic bottleneck]

Bioconversion of cellulosic biomass to ethanol is attracting much attention worldwide to help reduce carbon dioxide emissions from fossil fuels. The main components of cellulosic biomass are cellulose and hemicellulose, which are degraded to glucose and xylose, respectively. Because xylose is the second most abundant sugar in hard wood and herbs, converting not only glucose but also xylose to ethanol could greatly reduce the cost of bioconversion of cellulosic biomass to ethanol.

Saccharomyces cerevisiae is highly effective for the production of ethanol from glucose and has been used in the fermentation industry for a long time. However, *S. cerevisiae* cannot naturally use xylose for growth and ethanol production. Thus, many researchers have tried to develop engineered *S. cerevisiae* strains that can convert xylose to ethanol. Heterologous expression of the xylose reductase (XR) and xylitol dehydrogenase (XDH) genes from the xylose fermenting yeast *Scheffersomyces stipitis* is often used to introduce xylose-fermenting ability into *S. cerevisiae* (1–3). However, since the yeast thus produced has foreign genes, it is regarded as a genetically modified organism (GMO) and subjected to controls and limitations when it is used, so the economic efficiency of ethanol production decreases. A possible solution to overcome this problem could be the application of “self-cloning” yeast. Self-cloning yeast does not contain heterologous genes, and consists only of genes from the organism itself and closely related species. Some countries (such as Japan) do not regard self-cloning yeast as a GMO (4), so diffusion prevention measures become unnecessary. Thus, the use of self-cloning yeast greatly contributes to reduction of ethanol production costs. This is an important point when manufacturing something with a low selling price, such as ethanol.

S. cerevisiae possesses genes encoding aldose reductase (*GRE3*) and XDH (*XYL2*) that are respectively homologous to the xylose-assimilating XR and XDH genes of *S. stipitis* (5,6). The possibility of creating self-cloning xylose-using *S. cerevisiae* with *GRE3* and *XYL2* has been demonstrated (7). While *XYL2* was not induced in the presence of xylose, *SOR1*, coding for a sorbitol dehydrogenase that also has XDH activity, was induced. Subsequently, we showed that *S. cerevisiae* could be given the ability to use xylose by overexpression of *GRE3* and *SOR1* (8). These are the only reports on

* Corresponding author at: Kyushu University, c/o School of Interdisciplinary Science and Innovation, Student Affairs, Center Building 1, 744 Motoima, Nishi-ku, Fukuoka-City 819-0395, Japan. Tel.: +81 92 642 6691; fax: +81 92 642 6744.

E-mail addresses: fukuda@brs.kyushu-u.ac.jp (A. Fukuda), kuriya@people.kobe-u.ac.jp (Y. Kuriya), jin.konishi@jxtg.com (J. Konishi), kozue.mutaguchi@jxtg.com (K. Mutaguchi), takeshi.uemura.922@jxtg.com (T. Uemura), daipon@agr.kyushu-u.ac.jp (D. Miura), okahon@brs.kyushu-u.ac.jp (M. Okamoto).

1389-1723/$ – see front matter
https://doi.org/10.1016/j.jbiosc.2018.10.020

creating self-cloning xylose-using *S. cerevisiae*. However, as the ethanol productivity of the self-cloning xylose-using *S. cerevisiae* is not sufficient to be commercially viable, further modification is needed.

Metabolic pathway simulation is one of the most successful and useful approaches for improving the productivity of industrially relevant microorganisms during their cultivation (9–12). Metabolic flux analysis (MFA) is a systematic method to assess the roles of individual steps in a metabolic pathway network. Previous studies on xylose-using yeast utilizing MFA and metabolic modeling have been reported (13,14), but all relate to GMOs. There is no precedent for MFA and metabolic pathway simulation of self-cloning xylose-using yeast. GMO yeast and self-cloning yeast have different genes used to metabolize xylose, and because of different coenzyme specificities, their metabolic behavior is considered to be different.

The ethanol yield from glucose is now close to the theoretical value in many strains, and there is little margin for further improvement. However, since the ethanol yield from xylose in self-cloning yeast is still low, this can be improved. In this study, we analyzed the culture supernatant and intracellular metabolites of self-cloning xylose-using *S. cerevisiae* in xylose culture and constructed a kinetic model of the ethanol production pathway from xylose. Then, we identified a metabolic bottleneck and manipulated a gene corresponding to the bottleneck. Furthermore, ethanol productivity was examined in glucose and xylose mixed culture. This is the first report on metabolic simulation of self-cloning xylose-using *S. cerevisiae*.

MATERIALS AND METHODS

Strain, media and culture conditions The strain used in this study was the industrial sake yeast *S. cerevisiae* Kyokai No. 7 (K7). For precultivation of yeast cells, YPD medium (yeast extract 10 g/L, peptone 20 g/L, glucose 20 g/L) was used. Batch fermentations were carried out in 500-mL baffled shaken flasks (with a filtered silicone plug to avoid ethanol evaporation) at 30°C with shaking at 140 rpm in YPD medium (pH 5.0). Each flask contained the indicated amount of glucose and/or xylose as the carbon source(s). The initial cell concentration was 2×10^8 cells/mL for flask fermentation. A 5-L scale jar fermentor (ABLE, Tokyo, Japan) with 3 L working volume was also used for batch fermentation to control the dissolved oxygen concentration at 0.2 ppm. The temperature was maintained at 30°C, and the pH was controlled at 5.0 through addition of 5 M NaOH. The culture was sparged with air at 50 mL/min. The initial cell concentration was 1×10^7 cells/mL for jar fermentation. Flask and jar fermentor fermentations were carried out twice each. Synthetic complete (SC) medium containing 6.7 g/L yeast nitrogen base was used for yeast transformant selection. *Escherichia coli* JM109 was used for cloning of plasmids and grown at 37°C with shaking at 140 rpm in LB medium (yeast extract 5 g/L, tryptone 10 g/L, NaCl 5 g/L).

Plasmid and strain construction Construction of the xylose assimilating gene expression cassette, XR, XDH and xylulose kinase (XKS) with a phosphoglycerate kinase (*PGK1*) promoter and a terminator, was described previously (8). The expression cassette with *Eco*RI and *Hin*dIII restriction sites was introduced into the multiple cloning site of pUC18 (Takara, Shiga, Japan) to create pUC-XYL. *XYL2* was amplified from the genomic DNA of strain K7 with a *Sma*I restriction site and introduced into *Sma*I-digested pUC18 to create pUC-XYL2. pUC-XYL and pUC-XYL2 were digested with *Eco*RI and *Hin*dIII, and *Apa*I respectively. The fragments were blunted and ligated to create pUC-XYL2-XYL-XYL2. pUC-XYL2-XYL-XYL2 was digested with *Sma*I and transformed into K7 to produce strain K7-XYL. Yeast transformation was carried out by the lithium acetate method (15). Transformants were selected on SC agar plates with xylose as the sole carbon source.

Construction of the alcohol dehydrogenase (*ADH1*) overexpression vector was as follows. A *PGK1* promoter and terminator, and *ADH1*, were respectively amplified from the genomic DNA of strain K7. The three fragments were ligated and introduced into the *Sma*I site of pAUR135 (Takara) to create pAUR135-ADH1. pAUR135-ADH1 was digested with *Stu*I and transformed into K7-XYL to produce strain K7-XYL-ADH1. For selection of transformants, 0.5 mg/L aureobasidin A (Takara) was added to YPD agar plates.

Analytical methods Cell density was measured by optical density measurement at 600 nm (OD600) using a UV1800 spectrophotometer (Shimadzu, Kyoto, Japan). Cell growth was calculated using a predetermined correlation with OD600.

Concentrations of glucose, xylose, ethanol, glycerol, xylitol, and acetate in culture supernatants were determined with a high-performance liquid chromatography system (Shimadzu) equipped with a SUGAR SP0810 column (Shodex, Tokyo, Japan) using water as the mobile phase at a flow rate of 0.8 mL/min and 80°C.

Intracellular metabolites were quantitated using liquid chromatography/triple-stage quadrupole mass spectrometry (LC-QqQ-MS). Metabolite analysis by LC-QqQ-MS was performed as previously described (16), and samples were prepared as follows. For quenching, 1 mL cell culture was injected into a 15-mL Falcon tube containing 5 mL pure methanol precooled to −20°C and mixed by inversion. Subsequently, samples were centrifuged at 15,000 ×*g* at −9°C for 2 min, and the supernatant was discarded. The pellets were washed with 3 mL precooled water and centrifuged at 15,000 ×*g* at −9°C for 2 min. Samples were stored at −80°C until metabolite extraction. For metabolite extraction, the pellets were resuspended in 1 mL 100% methanol containing 6 μM (+)-10-camphor sulfonic acid (Tokyo Chemical Industry, Tokyo, Japan) as an internal standard and transferred to a 1.5-mL tube that contained 2 mm zirconia beads. The cell suspension was disrupted using a bead cell disrupter (MS-100R; TOMY, Tokyo, Japan) at 3000 rpm and −9°C for 5 min. Then, samples were centrifuged at 15,000 ×*g* at −9°C for 5 min, and supernatants were collected in a fresh 15-mL Falcon tube on ice. The pellets were resuspended in 1 mL 50% (v/v) methanol and disrupted again. Samples were centrifuged, and supernatants were added to the Falcon tube containing the methanol extract already recovered. The collected supernatants were mixed with chloroform and water at a ratio of 1:1.5:1 and centrifuged at 15,000 ×*g* at −9°C for 5 min. The aqueous phase of the extract was dried under vacuum (CVE-2000, EYELA, Tokyo and DTU-20, ULVAC, Kanagawa, Japan) and stored at −80°C until further use.

Model development A mathematical model of ethanol production from xylose in xylose-assimilating *S. cerevisiae* was constructed by an ordinary differential equation system with reference to previously reported models (17–19). As Fig. 1 shows, the metabolic model includes the central carbon metabolism system, pentose phosphate pathway, xylose metabolism pathway, and glycerol, ethanol and acetic acid production pathways. The mathematical model consists of two compartments: extracellular (culture fluid) and intracellular (cytoplasm). The intracellular metabolic reactions were described based on each enzyme reaction mechanism (20) (Table S1). Sugar uptake was described by a Michaelis–Menten type equation based on the difference in concentration inside and outside the cell (21,22). Substance transport between the two compartments was described via linear equations. Concentration change in each compartment because of the transport of substances inside and outside the cell was determined based on the yeast-specific cell volume 2.0 mL/g-dry cell weight (23) (Table S2). Among the coenzymes included in the model, ATP, ADP, AMP, NAD^+, NADH, $NADP^+$ and NADPH concentrations were interpolated from experimental time course data and used in simulation by substituting the values calculated by interpolation at each time point into other ordinary differential equations (Table S3 and Fig. S1). Quinone, quinol, CoA, phosphoric acid and CO_2 were assumed to be constant regardless of time (Table S2).

First, the kinetic parameter values for the mathematical model were investigated in enzyme reaction databases such as BRENDA (24), and as many kinetic parameter values as possible were acquired (Table S4). Next, other parameters whose values were unknown were estimated using a real-valued genetic algorithm (25) and manual operation to reproduce the experimental data obtained in flask culture with an initial xylose concentration of 50 g/L. Simulations were carried out with the Gear method (26) (Table S5). The simulation results of the model were evaluated by comparison with the time course of the experimental results and the correlation coefficient between the experimental values and the simulation values. Three mutants of K7-XYL, a xylulose kinase (*XKS1*) upregulation strain, a pyruvate decarboxylase (*PDC1*) upregulation strain, and a pyruvate transporter downregulation strain, were created to prevent overfitting in kinetic parameter estimation. The correlation coefficient between the experimental values and the simulation values of three mutants are shown in Table S6. A *XKS1* upregulation strain and a *PDC1* upregulation strain were constructed in the same method for preparing an *ADH1* upregulation strain described in the materials and methods. A pyruvate transporter downregulation strain was substituted by a pyruvate dehydrogenase (*PDA1*) downregulation strain, which was created by disruption of *PDA1*, since it was difficult to disrupt pyruvate transporter itself. The mathematical equations for the ethanol production system, kinetic parameters, and initial values of dependent variables are described in the supplemental materials (Tables S1–S5).

Sensitivity analysis Sensitivity analysis is a method for assessing the validity of a developed model and clarifying which pathway(s) have the most impact, in the present case on ethanol productivity. The amount of ethanol production at 48 h was assessed in this study because all the xylose was consumed by 48 h.

The endpoint deviation (ED) of ethanol described below was assessed to reveal which reaction pathway(s) impact ethanol production. In this calculation, we assigned a 100% increase to each kinetic parameter in rate equations in the model; each kinetic parameter was tested individually in this way.

$$ED = 100 \times ([Ethanol]_{change} - [Ethanol]_{control})/[Ethanol]_{control} \quad (1)$$

where $[Ethanol]_{change}$ was the ethanol concentration at 48 h given a 100% increase in the kinetic parameter in the rate equation, and $[Ethanol]_{control}$ was the ethanol concentration without any change. The higher the absolute value of ED, the more a

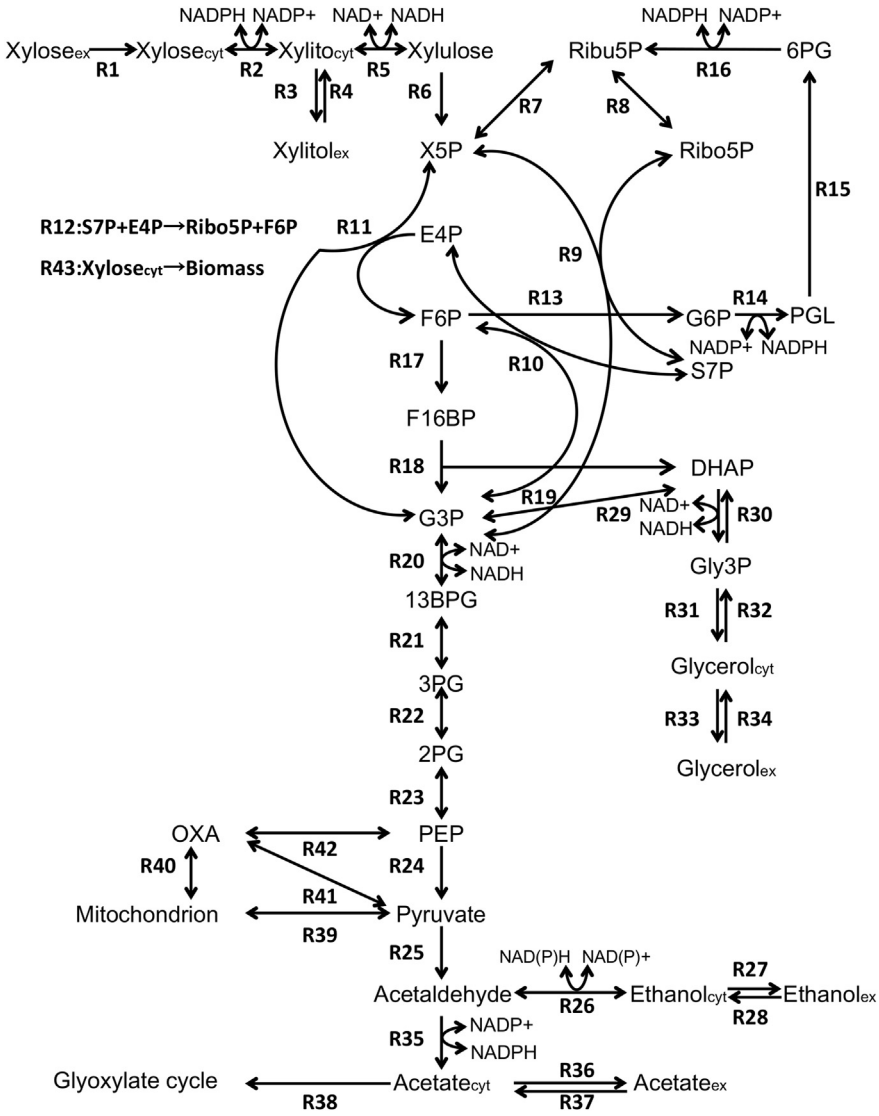

FIG. 1. Metabolic pathway of ethanol production from xylose. X5P, xylulose 5-phosphate; Ru5P, ribulose 5-phosphate; R5P, ribose 5-phosphate; S7P, sedoheptulose 7-phosphate; GAP, glyceraldehyde 3-phosphate; E4P, erythrose 4-phosphate; F6P, fructose 6-phosphate; G6P, glucose 6-phosphate; PGL, 6-phosphogluconolactone; 6PG, 6-phosphogluconate; FBP, fructose-1, 6-bisphosphate; 1,3BPG, 1,3-bisphosphoglycerate; 3PG, glycerate 3-phosphate; 2PG, glycerate 2-phosphate; PEP, phosphoenolpyruvic acid; DHAP, dihydroxyacetone phosphate; Gly3P, glycerol 3-phosphate; OXA, oxaloacetic acid.

kinetic parameter affects the ethanol production. Various genetic manipulation strategies were developed based on the outcomes of this analysis.

RESULTS

Development of the kinetic simulation model of the ethanol production pathway Batch cultures of strain K7-XYL were grown in 500-mL baffled shaken flasks with an initial xylose concentration of 50 g/L to obtain experimental data in preparation for the development of the kinetic simulation model of ethanol production. The experimental time course data and simulation results are shown in Fig. 2. The xylose was depleted after 48 h and the ethanol concentration reached 12.6 g/L at 24 h. The simulation was conducted using an original program developed in the language C. Forty-three reactions and 46 metabolites were included in the model (Tables S1 and S5). The metabolic concentration data and the initial metabolic state were determined based on data we acquired in this study. The model included allosteric regulation of 6-phosphofructokinase and pyruvate kinase based on previous works (17,19). The cell growth rate equation included a term for growth shut-down to avoid excess growth in the simulation. For coenzymes, time-course data of the coenzyme concentrations obtained by measurement were interpolated and expressed as a function of time. Constraints such as competitive inhibition by substrate(s) and/or product(s) and equilibrium constants were included based on enzyme kinetics and reactions. The correlation coefficients (r) between the experimental data and the simulation results for each metabolite were calculated to be: 0.999 for xylose, 0.953 for xylitol, 0.997 for glycerol, 0.999 for ethanol, 0.991 for biomass, and 0.927 for acetate; overall, r was 0.978. To avoid overfitting in kinetic parameter estimation, three mutants of K7-XYL, a *XKS1* upregulation strain, a *PDC1* upregulation strain, and a pyruvate transporter downregulation strain, were created. The kinetic parameters of the model were changed in one place to correspond to each of the three mutations, and simulation was carried out. The simulation results agreed with experimental data in the three mutants as shown in Table S6. We conducted sensitivity analysis using this simulation model and parameter

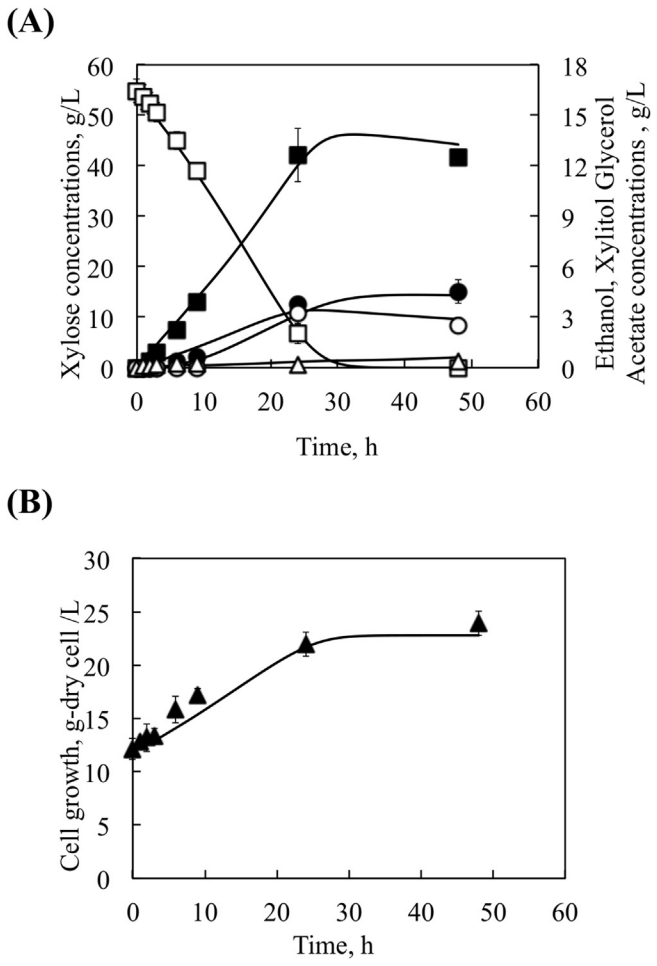

FIG. 2. Experimental time course data and simulation results with initial xylose concentration 50 g/L. The symbols show experimental data and the lines indicate simulation results. Experimental results are based on two replications. Data points represent the average of two experiments and error bars indicate standard deviations. (A) Xylose, open squares; ethanol, closed squares; xylitol, open circles; glycerol, closed circles; acetate, open triangles. (B) Biomass, closed triangles.

sets, since the correlation coefficients of the simulation results and experimental data were consistent for the three mutants of K7-XYL.

Sensitivity analysis Our top three ranked sensitivity analysis results and genetic manipulation strategies are shown in Table 1. Table S7 shows the ED values of reactions having the fourth or less impact onward on ethanol production and two of our prediction results were compared with the previous metabolic engineering works of the xylose-using *S. cerevisiae* strains in Table S7. The factor in our simulation that had the biggest effect on ethanol production was upregulation of XDH (R5 in Fig. 1). However, XDH has already been upregulated with the *PGK1* promoter to add xylose using ability to the yeast (K7-XYL). Since the *PGK1* promoter is one of the strongest promoters in *S. cerevisiae* (27), we decided that further upregulation of XDH would be difficult. As our simulation showed other strategies that would lead to high ED values, no further upregulation of XDH was undertaken in this study.

The second ranked reaction that had an impact on ethanol production was downregulation of xylose uptake (R1 in Fig. 1). However, there is no xylose-specific transporter in *S. cerevisiae*, and it is considered that non-specific hexose transporters transport xylose with low transport rates (28,29). Thus, downregulation of xylose uptake is not feasible within the constraints of our experiments (i.e., in self-cloning xylose-using *S. cerevisiae*).

The third ranked enzyme reaction that had an impact on ethanol production was that of alcohol dehydrogenase (R26 in Fig. 1). Our simulation suggested that if ADH was upregulated twofold, the ethanol productivity would increase by about 13%. We decided to upregulate ADH and examine the effect on ethanol productivity, because this manipulation strategy was feasible and logical.

Effect of *ADH1* overexpression in xylose medium and glucose/xylose mixed medium Initially, flask-scale cultures of strains K7-XYL and K7-XYL-ADH1 were grown in 500-mL baffled shaken flasks with an initial xylose concentration of 50 g/L (Fig. 3A and B). Although K7-XYL-ADH1 converted xylose to ethanol slightly slower than K7-XYL (K7-XYL 1.31 g/L/h, K7-XYL-ADH1 1.08 g/L/h), the ethanol productivity of strain K7-XYL-ADH1 was higher than that of K7-XYL (K7-XYL 12.5 g/L, K7-XYL-ADH1 13.8 g/L). Glycerol production by K7-XYL-ADH1 increased by 0.73 g/L, and xylitol production of K7-XYL-ADH1 decreased by 4.01 g/L relative to strain K7-XYL, respectively. The productivity of xylitol in Fig. 2A was about half of that in Fig. 3A, because the amount of liquid in the flask used to generate the data in Fig. 2A became less than that in the flask used for Fig. 3A, so conditions in Fig. 2A were more aerobic and accumulation of xylitol was suppressed. This was because, in order to obtain data for model construction, the sampling frequency in Fig. 2A was higher than that in Fig. 3A. Furthermore, for the collection of intracellular metabolite data, the sampling amount in Fig. 2A was large. It was difficult to reproduce reduction of liquid volume by sampling in the simulation. The ethanol yield from the initial sugars was 46.5% for strain K7-XYL and 51.1% for K7-XYL-ADH1, which indicated that overexpression of *ADH1* increased the ethanol yield in xylose medium.

Second, the effect of *ADH1* overexpression in medium containing a mixture of glucose and xylose was evaluated. K7-XYL consumed glucose first, then fermented xylose after depletion of glucose. Since K7-XYL does not simultaneously consume glucose and xylose, we expected that the effect of *ADH1* overexpression would be observed in glucose and xylose mixed medium during the xylose consumption phase. Fig. 3C and D shows culture parameters for flask scale cultures of K7-XYL and K7-XYL-ADH1 with YP (yeast extract 10 g/L, peptone 20 g/L) medium containing glucose (initial concentration 80 g/L) and xylose (initial concentration 50 g/L), representing the typical sugar composition of cellulosic biomass. Both strains rapidly fermented glucose to ethanol and then fermented xylose. As observed in xylose medium, the xylose consumption rate of K7-XYL-ADH1 was slower than that of K7-XYL.

TABLE 1. Top three ranked manipulation strategy for higher production of ethanol.

Rank	Reaction step[a]	Strategy	Enzyme[b]	Sensitivity, %[c]	Reaction
1	R5	Up	XDH	16.4	$Xylitol_{cyt} \rightarrow NAD^+ \Leftrightarrow Xylulose + NADH$
2	R1	Down	Xylose uptake	13.3	$Xylose_{ex} \rightarrow Xylose_{cyt}$
3	R26	Up	ADH	13.2	$Acetaldehyde + NAD(P)H \rightarrow Ethanol_{cyt} + NAD(P)^+$

[a] Reaction step corresponds to numbering in Fig. 1.
[b] Enzymes are abbreviated as follows: XDH, xylose dehydrogenase; ADH, alcohol dehydrogenase.
[c] Sensitivity indicates the endpoint deviation (ED) of ethanol at 48 h, when we applied a 100% increase to each respective kinetic parameter in the rate equations in the model.

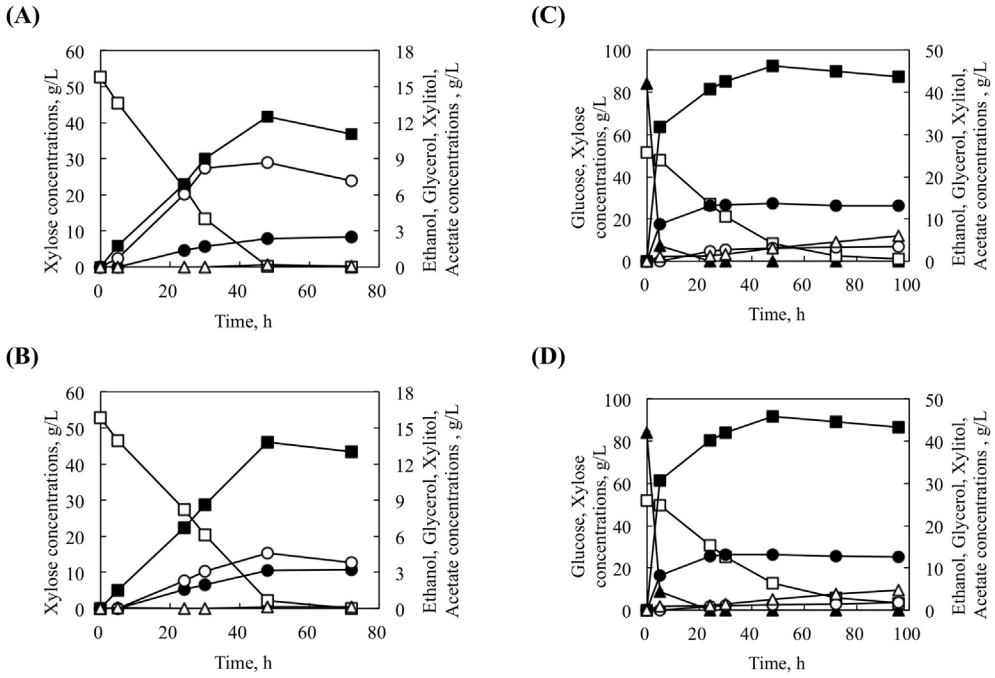

FIG. 3. Fermentation profiles of flask cultures of strains K7-XYL (A, C) and K7-XYL-ADH1 (B, D) in YP medium containing 50 g/L xylose (A, B) or 80 g/L glucose plus 50 g/L xylose (C, D) as the carbon source(s). Results are based on two replications. Data points represent the average of two experiments and error bars indicate standard deviations. Glucose, closed triangles; xylose, open squares; ethanol, closed squares; xylitol, open circles; glycerol, closed circles; acetate, open triangles.

However, the ethanol productivity of K7-XYL-ADH1 was almost the same as that of K7-XYL in the glucose and xylose mixed-medium (K7-XYL 46.3 g/L, K7-XYL-ADH1 45.9 g/L). These data indicated that, unlike in xylose medium, overexpression of *ADH1* did not increase the ethanol yield in glucose and xylose mixed medium in flask-scale culture.

Controlled dissolved oxygen fermentation In flasks, although an effect of *ADH1* overexpression was observed when xylose was the sole carbon source, the effect was not confirmed in mixed glucose-xylose medium. We presumed that the internal redox balance of the cells changed due to the presence of the glucose and this led to there being no effect of *ADH1* overexpression. To modify the internal redox balance, 5-L jar fermentor cultures of K7-XYL and K7-XYL-ADH1 were grown with dissolved oxygen concentration maintained at 0.2 ppm. Fig. 4 shows the culture parameters. Both strains converted 80 g/L glucose and 50 g/L xylose within 48 h. Although the initial cell concentration in the 5-L jar fermentor culture was 20-times lower than that in flask-scale cultures, xylose consumption in the 5-L jar fermentor was faster than that in flask-scale culture. The ethanol productivity of strain K7-XYL-ADH1 was higher than that of K7-XYL (K7-XYL 44.9 g/L, K7-XYL-ADH1 49.2 g/L). The ethanol yield from the initial sugars was 66.9% for K7-XYL, and 73.3% for K7-XYL-ADH1. The results from the 5-L jar fermentor with controlling oxygen concentration sufficiently reflect the results of their flask culture, even though the amount of medium was significantly different between the flask cultivation and the 5-L jar fermentor.

DISCUSSION

We analyzed an ethanol production pathway of *S. cerevisiae* involving the endogenous xylose-assimilating genes *GRE3* and *SOR1* (i.e., a self-cloning xylose-using *S. cerevisiae*) by construction of a kinetic simulation model of the ethanol producing pathway and undertaking sensitivity analysis in that model. Then, we identified a metabolic bottleneck in the pathway. Analysis revealed that the reaction catalyzed by ADH1 was a bottleneck, and that overexpression of *ADH1* would enable the self-cloning xylose-using *S. cerevisiae* to increase the ethanol yield. This was verified in the presence of xylose in flask-scale cultures (K7-XYL, yield 12.5 g/L; K7-XYL-ADH1, 13.8 g/L), and in the presence of glucose and xylose in 5-L jar fermentor cultures (K7-XYL, yield 45.0 g/L; K7-XYL-ADH1 49.4 g/L). Improvement in ethanol yield by 10% means that variable and fixed costs are reduced by 10%. That would have a dynamic impact on industry, especially in manufacture of a low-priced product such as ethanol. Natural cellulosic biomass contains both glucose and xylose. The ethanol yield (g ethanol/g sugars) from strain K7-XYL-ADH1 was 0.38 in the presence of glucose and xylose in 5-L jar fermentor culture. By comparison, the ethanol yield from genetically modified yeasts containing *S. stipitis* XR and XDH was 0.40 (30,31). Thus, our self-cloning yeast showed almost same the ethanol productivity as genetically modified yeast. In the future, overexpression of ADH1 should be carried out in genetically modified yeast and the effect on ethanol productivity should be confirmed. If there is a positive effect on genetically modified yeast, a quantitative comparison with self-cloning yeast is necessary.

S. stipitis XR can use both NADPH and NADH. However, GRE3 has strict NADPH specificity (32). *S. stipitis* XDH and SOR1 use only NAD^+ as a cofactor, but self-cloning xylose-using *S. cerevisiae* containing GRE3 cannot supply NAD^+ for the XDH reaction. That is, the metabolic pathways in the self-cloning xylose-using *S. cerevisiae* tend to cause a cofactor imbalance. Creating a self-cloning xylose-using *S. cerevisiae* is difficult (as mentioned above), but would be expected to contribute to the reduction of ethanol production costs. In oxygen-controlled fermentation conditions, our self-cloning xylose-using *S. cerevisiae* showed close to the same ethanol yield as the genetically modified yeast, suggesting that there is a possibility that self-cloning xylose-using *S. cerevisiae* could be used for industrial ethanol production. Strain K7-XYL-ADH1 showed higher ethanol yield than K7-XYL in the presence of glucose and xylose in 5-L jar fermentor culture but not in flask culture. We guessed that

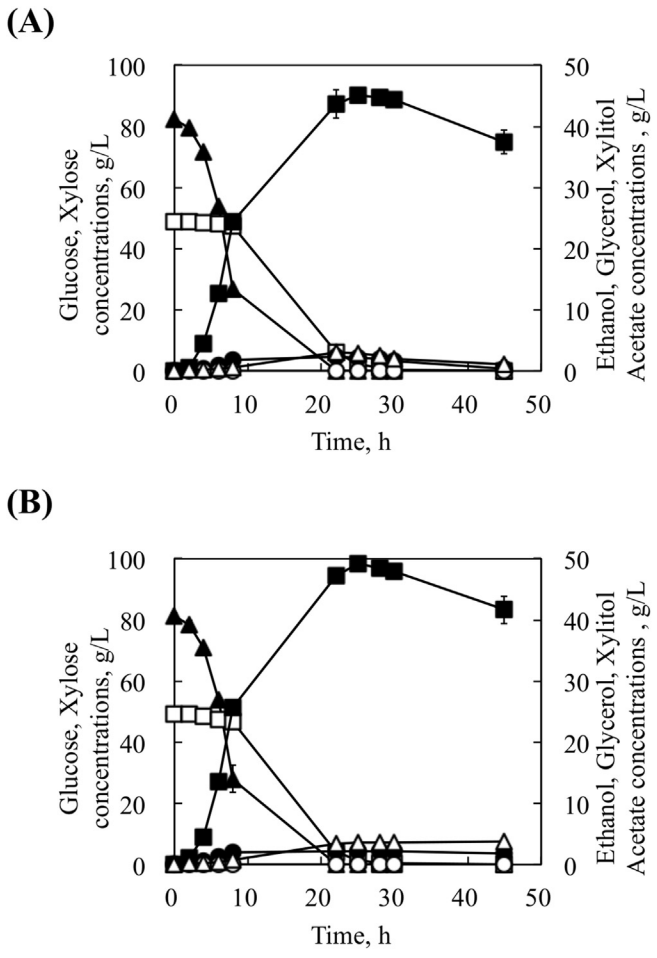

FIG. 4. Fermentation profiles of 5-L jar fermentor cultures of strains K7-XYL (A) and K7-XYL-ADH1 (B) in YP medium containing 80 g/L glucose plus 50 g/L xylose as carbon sources. Results are based on two replications. Data points represent the average of two experiments and error bars indicate standard deviations. Glucose, closed triangles; xylose, open squares; ethanol, closed squares; xylitol, open circles; glycerol, closed circles; acetate, open triangles.

this was because, in flask culture, the dissolved oxygen concentration was low during the xylose consumption phase because most of the oxygen had been consumed during the glucose consumption phase, and, due to lack of respiration, NAD^+ regeneration did not occur. Therefore, the NAD^+ supply was not sufficient for the reaction of XDH. The increased oxygen supply in the aerated 5-L jar fermentor might make it possible to regenerate NAD^+ by respiration and thus accelerate the conversion of xylitol to xylulose by XDH, leading to an overall increase in ethanol production. Since only one oxygen concentration was tested in our experiments, ethanol productivity may increase further if the oxygen concentration is optimized.

We constructed a kinetic model of ethanol production from xylose and conducted a sensitivity analysis to assess the validity of the model and clarify which pathway(s) have most impact on the ethanol productivity. The model we constructed identified a bottleneck in the ethanol production pathway. Since our experimental data were consistent with the prediction, the method was validated. Although we have not implemented MFA this time, we believe that it is necessary to compare MFA of self-cloning yeast with that of genetically modified yeast to further improve ethanol productivity in the future.

In summary, we have demonstrated that overexpression of *ADH1* in *S. cerevisiae* strain K7-XYL improved ethanol productivity in glucose and xylose mixed medium. Our xylose-using *S. cerevisiae* had almost the same ethanol productivity as genetically modified yeast, despite the large constraint of self-cloning. From the viewpoint of industrialization of ethanol conversion from cellulosic biomass, use of self-cloning yeast is an important approach to increase ethanol productivity without using GMOs.

Supplementary data to this article can be found online at https://doi.org/10.1016/j.jbiosc.2018.10.020.

ACKNOWLEDGMENTS

This work was supported by the New Energy and Industrial Technology Development Organization, Japan (Development of an Innovative and Comprehensive Production System for Cellulosic Bioethanol, project code: P09014).

References

1. **Kötter, P. and Ciriacy, M.:** Xylose fermentation by *Saccharomyces cerevisiae*, Appl. Microbiol. Biotechnol., **38**, 776–783 (1993).
2. **Ho, N. W., Chen, X., and Brainard, A. P.:** Genetically engineered *Saccharomyces* yeast capable of effective cofermentation of glucose and xylose, Appl. Environ. Microbiol., **64**, 1852–1859 (1998).
3. **Karhumaa, K., Fromanger, R., Hahn-Hägerdal, B., and Gorwa-Grauslund, M. F.:** High activity of xylose reductase and xylitol dehydrogenase improves xylose fermentation by recombinant *Saccharomyces cerevisiae*, Appl. Microbiol. Biotechnol., **73**, 1039–1046 (2007).
4. **Hino, A.:** Safety assessment and public concerns for genetically modified food products: the Japanese experience, Toxicol. Pathol., **30**, 126–128 (2002).
5. **Träff, K. L., Jönsson, L. J., and Hahn-Hägerdal, B.:** Putative xylose and arabinose reductases in *Saccharomyces cerevisiae*, Yeast, **19**, 1233–1241 (2002).
6. **Richard, P., Toivari, M. H., and Penttilä, M.:** Evidence that the gene YLR070c of *Saccharomyces cerevisiae* encodes a xylitol dehydrogenase, FEBS Lett., **457**, 135–138 (1999).
7. **Toivari, M. H., Salusjärvi, L., Ruohonen, L., and Penttilä, M.:** Endogenous xylose pathway in *Saccharomyces cerevisiae*, Appl. Environ. Microbiol., **70**, 3681–3686 (2004).
8. **Konishi, J., Fukuda, A., Mutaguchi, K., and Uemura, T.:** Xylose fermentation by *Saccharomyces cerevisiae* using endogenous xylose-assimilating genes, Biotechnol. Lett., **37**, 1623–1630 (2015).
9. **Bailey, J. E.:** Toward a science of metabolic engineering, Science, **252**, 1668–1675 (1991).
10. **Stephanopoulos, G. and Vallino, J. J.:** Network rigidity and metabolic engineering in metabolite overproduction, Science, **252**, 1675–1681 (1991).
11. **Vallino, J. J. and Stephanopoulos, G.:** Metabolic flux distributions in *Corynebacterium glutamicum* during growth and lysine overproduction, Biotechnol. Bioeng., **41**, 633–646 (1993).
12. **Kuriya, Y., Tanaka, S., Kobayashi, G., Hanai, T., and Okamoto, M.:** Development of an analytical pipeline for optimizing substrate feeding and eliminating metabolic bottlenecks, Chem. Bio Inf. J., **11**, 1–23 (2011).
13. **Wasylenko, T. M. and Stephanopoulos, G.:** ^{13}C-Metabolic flux analysis of a xylose-consuming *Saccharomyces cerevisiae* strain expressing xylose isomerase, Biotechnol. Bioeng., **112**, 470–483 (2015).
14. **Parachin, N. S., Bergdahl, B., van Niel, E. W. J., and Gorwa-Grauslund, M. F.:** Kinetic modelling reveals current limitations in the production of ethanol fro xylose by recombinant *Saccharomyces cerevisiae*, Metab. Eng., **13**, 508–517 (2011).
15. **Giets, D., St Jean, A., Woods, R. A., and Schiestl, S. H.:** Improved method for high efficiency transformation of intact yeast cells, Nucleic Acids Res., **20**, 1425 (1992).
16. **Kiyonari, S., Iimori, M., Matsuoka, K., Watanabe, S., Morikawa-Ichinose, T., Miura, D., Niimi, S., Saeki, H., Tokunaga, E., Oki, E., and other 3 authors:** The 1,2-diaminocyclohexane carrier ligand in oxaliplatin induces p53-dependent transcriptional repression of factors involved in thymidylate biosynthesis, Mol. Canc. Therapeut., **14**, 2332–2342 (2015).
17. **Teusink, B., Passarge, J., Reijenga, C. A., Esgalhado, E., van der Weijden, C. C., Schepper, M., Walsh, M. C., Bakker, B. M., van Dam, K., Westerhoff, H. V., and Snoep, J. L.:** Can yeast glycolysis be understood in terms of in vitro kinetics of the constituent enzymes? Testing biochemistry, Eur. J. Biochem., **267**, 5313–5329 (2000).
18. **Hynne, F., Danø, S., and Sørensen, P. G.:** Full-scale model of glycolysis in *Saccharomyces cerevisiae*, Biophys. Chem., **94**, 121–163 (2001).
19. **Rizzi, M., Baltes, M., Theobald, U., and Reuss, M.:** In vivo analysis of metabolic dynamics in *Saccharomyces cerevisiae*: II. Mathematical model, Biotechnol. Bioeng., **55**, 592–608 (1997).

20. **Cleland, W. W.:** The kinetics of enzyme-catalyzed reactions with two or more substrates or products: I. Nomenclature and rate equations, Biochim. Biophys. Acta, **67**, 104–137 (1963).
21. **Bertilsson, M., Andersson, J., and Lidén, G.:** Modeling simultaneous glucose and xylose uptake in *Saccharomyces cerevisiae* from kinetics and gene expression of sugar transporters, Bioproc. Biosyst. Eng., **31**, 369–377 (2008).
22. **Teusink, B., Diderich, J. A., Westerhoff, H. V., van Dam, K., and Walsh, M. C.:** Intracellular glucose concentration in derepressed yeast cells consuming glucose is high enough to reduce the glucose transport rate by 50%, J. Bacteriol., **180**, 556–562 (1998).
23. **Van Urk, H., Mak, P. R., Scheffers, W. A., and van Dijken, J. P.:** Metabolic responses of *Saccharomyces cerevisiae* CBS 8066 and *Candida utilis* CBS 621 upon transition from glucose limitation to glucose excess, Yeast, **4**, 283–291 (1988).
24. **Schomburg, I., Chang, A., Placzek, S., Söhngen, C., Rother, M., Munaretto, C., Stelzer, M., Grote, A., Scheer, M., and Schomburg, D.:** BRENDA in 2013: integrated reactions, kinetic data, enzyme function data, improved disease classification: new options and content in BRENDA, Nucleic Acids Res., **41**, D764–D772 (2013).
25. **Akimoto, Y., Nagata, Y., Sakuma, J., Ono, I., and Kobayashi, S.:** Proposal and evaluation of adaptive real-coded crossover AREX, Trans. Jpn. Soc. Artif. Intell., **24**, 446–458 (2009).
26. **Gear, C. W.:** Numerical initial value problem in ordinary differential equations. Prentice-Hall, Upper Saddle River (1971).
27. **Partow, S., Siewers, V., Bjørn, S., Nielsen, J., and Maury, J.:** Characterization of different promoters for designing a new expression vector in *Saccharomyces cerevisiae*, Yeast, **27**, 955–964 (2010).
28. **Lee, W. J., Kim, M. D., Ryu, Y. W., Bisson, L. F., and Seo, J. H.:** Kinetic studies on glucose and xylose transport in *Saccharomyces cerevisiae*, Appl. Microbiol. Biotechnol., **60**, 186–191 (2002).
29. **Saloheimo, A., Rauta, J., Stasyk, O. V., Sibirny, A. A., Penttila, M., and Ruohonen, L.:** Xylose transport studies with xylose-utilizing *Saccharomyces cerevisiae* strains expressing heterologous and homologous permeases, Appl. Microbiol. Biotechnol., **74**, 1041–1052 (2007).
30. **Matsushika, A. and Sawayama, S.:** Effect of initial cell concentration on ethanol production by flocculent *Saccharomyces cerevisiae* with xylose-fermenting ability, Appl. Biochem. Biotechnol., **162**, 1952–1960 (2010).
31. **Casey, E., Sedlak, M., Ho, N. W. Y., and Mosier, N. S.:** Effect of acetic acid and pH on the cofermentation of glucose and xylose to ethanol by a genetically engineered strain of *Saccharomyces cerevisiae*, FEMS Yeast Res., **10**, 385–393 (2010).
32. **Kuhn, A., van Zyl, C., van Tonder, A., and Prior, B. A.:** Purification and partial characterization of aldo-keto reductase from *Saccharomyces cerevisiae*, Appl. Environ. Microbiol., **61**, 1580–1585 (1995).